Published in final edited form as:
Ann Biomed Eng. 2014 March ; 42(3): 619–630. doi:10.1007/s10439-013-0915-2.

The Tendon Injury Response Is Influenced by Decorin and Biglycan

Andrew A. Dunkman[a], **Mark R. Buckley**[a], **Michael J. Mienaltowski**[b], **Sheila M. Adams**[b], **Stephen J. Thomas**[a], **Lauren Satchell**[a], **Akash Kumar**[a], **Lydia Pathmanathan**[a], **David P. Beason**[a], **Renato V. Iozzo**[c], **David E. Birk**[b], and **Louis J. Soslowsky**[+,a]

[a]The McKay Orthopaedic Research Laboratory, University of Pennsylvania, 424 Stemmler Hall, 3450 Hamilton Walk, Philadelphia, PA 19104, USA

[b]Department of Molecular Pharmacology & Physiology, University of South Florida Morsani College of Medicine, 12901 Bruce B. Downs Blvd, MDC 8, Tampa FL, 33612, USA

[c]Department of Pathology, Anatomy & Cell Biology, Thomas Jefferson University, 1020 Locust Street, Jefferson Alumni Hall, Suite 249. Philadelphia, PA, 19107

Abstract

Defining the constituent regulatory molecules in tendon is critical to understanding the process of tendon repair and instructive to the development of novel treatment modalities. The purpose of this study is to define the structural, expressional, and mechanical changes in the tendon injury response, and elucidate the roles of two class I small leucine-rich proteoglycans (SLRPs). We utilized biglycan-null, decorin-null and wild type mice with an established patellar tendon injury model. Mechanical testing demonstrated functional changes associated with injury and the incomplete recapitulation of mechanical properties after six weeks. In addition, SLRP deficiency influenced the mechanical properties with a marked lack of improvement between three and six weeks in decorin-null tendons. Morphological analyses of the injury response and role of SLRPs demonstrated alterations in cell density and shape as well as collagen alignment and fibril structure resulting from injury. SLRP gene expression was studied using RT-qPCR with alterations in expression associated with the injured tendons. Our results show that in the absence of biglycan initial healing may be impaired while in the absence of decorin later healing is clearly diminished. This suggests that biglycan and decorin may have sequential roles in the tendon response to injury.

Key Terms

Tendon; Injury; Biglycan; Decorin; Proteoglycan; Extracellular Matrix; SLRP; healing

Introduction

As the conduits of force transfer from muscle to bone, tendons are susceptible to injury in a myriad of activities. Although an injured tendon can mount a significant reparative response, incomplete recapitulation of pre-injury functionality is well documented. In healthy tendon, collagen fibrils, the primary structural components of tendon, are organized in uniaxially arranged bundles called fibers. After healing from an injury, new tissue is structurally and mechanically inferior to uninjured tissue.[19] Multiple factors, including small leucine rich

Corresponding Author: Louis J. Soslowsky, McKay Orthopaedic Research Laboratory, University of Pennsylvania, 424 Stemmler Hall, 3450 Hamilton Walk, Philadelphia, PA 19104, Tel.: (215) 898-8653; Fax: (215) 573-2133; soslowsk@upenn.edu.

proteoglycans (SLRPSs) and their associated glycosaminoglycan (GAG) chains, influence the organization of collagen in tendon.[9,10,12,14,29] Gaining insight into these regulators is instructive to the development of novel treatment modalities for tendon injury and pathology.

Decorin and biglycan are the principal small leucine rich proteoglycans (SLRPs) in tendon, and contain one or two chondroitin sulfate GAG chains, respectively.[17] Researchers have examined the influence of these molecules on development[3,25,30], mechanics[12] and aging.[14] SLRPs' roles as mediators of collagen fibril assembly and growth in multiple tissues have been supported by numerous investigations.[1,8,25,26,27,28] The tendons of SLRP deficient animals have been shown to be mechanically inferior [12,13,27] In tendons, biglycan expression is upregulated after injury[4,21] and decorin expression is initially downregulated.[4] However, although we know that SLRP expression changes with injury, the temporal, structural and mechanical influences of decorin and biglycan in tendon healing are not yet understood.

The objective of this study was to investigate the roles of decorin and biglycan in tendon healing using wild type (WT), biglycan-null ($Bgn^{-/-}$) and decorin-null ($Dcn^{-/-}$) mouse models. Using an established patellar tendon injury model, we examined structural, expressional, and mechanical changes induced by the deficiency of specific SLRPs. We compared two post-injury times points—three weeks and six weeks to uninjured tendons across the three genotypes. We hypothesized that decorin-null and biglycan-null tendons would exhibit an inferior repair response compared to wild type.

Materials and Methods

A total of 136 female wild-type (WT), biglycan transgenic null ($Bgn^{-/-}$), and decorin transgenic null ($Dcn^{-/-}$) mice were used in this study with approval from The University of Pennsylvania and University of South Florida's Institutional Animal Care and Use Committees. All mice were on a C57BL6 background. At approximately 120 days of age, two thirds of the animals in each genotype underwent bilateral surgery under aseptic conditions as previously described.[20] Briefly, a single incision was made in the skin near the knee, and longitudinal incisions were made adjacent to and on either side of the patellar tendon. A rubber-coated backing was placed under the tendon and a full thickness, partial width (~60%) region of the tendon was transected with a 0.75mm biopsy punch. Skin was sutured and the animals were allowed to return to cage activity. They were then sacrificed at three or six weeks post-injury. Additional animals were sacrificed at 150 days (equal to 120 days plus 4.5 weeks, splitting the difference between injury groups and thus minimizing unnecessary animal sacrifice) to serve as uninjured controls.

Immediately after sacrifice, one hind limb of each animal was wrapped in gauze, soaked in phosphate buffered saline (PBS), and frozen for later mechanical testing. From the contralateral limb, the tendon was longitudinally bisected through the injury and randomly assigned to two of three additional assays to further analyze the injury site: RT-qPCR, transmission electron microscopy (TEM), and histology.

Mechanical Testing

In preparation for mechanical testing, frozen hind limbs were thawed and all surrounding musculature and soft tissue was removed to isolate the tibia-patellar tendon-patella complex. The tendon was stamped into "dog-bone" shape [S-Figure 3], effectively isolating the repair tissue from the uninjured struts. A custom laser device was used to take 5 measurements of cross sectional area across the midsection of the stamped region and these were averaged.[16] The tibia was then potted in acrylic, speckle coated with Verheoff's stain for optical

tracking, and loaded into an Instron 5848 (Instron, Natick, MA) universal testing system with custom fixtures. Throughout preparation, the tendon was kept hydrated with PBS and was tested submerged in a PBS bath maintained at 37°C.

The mechanical testing procedure consisted of a modified version of an established protocol[12,14,22] consisting of 1) preconditioning 2) stress-relaxation and frequency sweep (0.01, 0.1, 1, 5, 10 Hz) at each 4%, 6%, and 8% strains and 3) return to gauge length and a 0.1%/s ramp-to-failure. Data was collected for 10 cycles per frequency and averaged. A 10 minute hold at each strain allowed the tendon to relax prior to dynamic oscillations. The ramp-to-failure was imaged at 2 frames per second.

The Instron controlled displacement and recorded both displacement and load. By dividing these parameters by gauge length and cross-sectional area, respectively, stress and strain sinusoids from cyclic loading were obtained. The dynamic modulus |E*| (defined by the ratio of the amplitudes of the stress and strain sinusoids and reported in MPa) was calculated for each strain-frequency combination. Likewise, the phase angle δ, the peak-to-peak distance (in degrees) between curves (resulting from the time lag between stress and strain) was obtained. The tangent of this value, tan δ, was calculated and is equal to the ratio of dissipated to stored energy. Additionally, the ramp to failure was analyzed with optical tracking software to obtain quasi-static properties including toe modulus, linear modulus, transition strain and transition stress.

Our dynamic testing protocol utilized 3 strains, 5 frequencies, 3 genotypes, and 3 injury states to examine two mechanical parameters. Although this comprehensive study design could, in concept, be analyzed by a four-way ANOVA with some factors as repeated measures and some as not, our specific hypotheses were best tested in a focused manner utilizing t-tests as previously described.[14] Specifically, t-tests are calculated for each frequency and strain level, across injury states within each genotype [Table 1] and then across genotypes within each injury state [Table 2]. In each analysis, each group was compared to two other groups, so to correct for multiple comparisons, significance was set at and $p \leq 0.05/2$ and $0.05/2 \leq p \leq 0.1/2$ was considered a trend. Inferences were made based upon consistent results.

RT-qPCR

Real-time quantitative polymerase chain reaction assay (RT-qPCR) was used to quantify expression levels for biglycan, decorin, lumican, and fibromodulin as previously described.[14] Briefly, individual tissue samples were mechanically homogenized with a Tissue-Tearor (Model 398, 467 Biospec Products, Inc., Bartlesville, OK) in QIAzol reagent (Qiagen, Valencia, CA). Total RNA was isolated by applying the QIAzol:chloroform supernatant to the RNeasy Micro Kit (Qiagen) using the manufacturer's protocol. Given the yields of total RNA from small amounts of tissue, to analyze expression from each individual sample, mRNA was amplified by Single Primer Isothermal Amplification (SPIA), a method shown to produce expression data that is highly correlative to non-amplified transcript data.[11] The mRNA of 25 ng of total RNA was reverse transcribed into cDNA and amplified using the WT-Ovation RNA Amplification System (NuGEN, San Carlos, CA). The resulting SPIA product was purified with a QIAquick PCR Purification Kit (Qiagen) and the amplified cDNA was eluted with 30 μl RNase-free water. For qPCR analysis, 1 μl of amplified cDNA template was added to a reaction volume of 20 μl per well in an ABI StepOnePlus Real-Time PCR System (Applied Biosystems, Foster City, CA) with a Fast SYBR Green Master Mix (Applied Biosystems). Mouse specific primers for β-actin (Actb: F — AGATGACCCAGATCATGTTTGAGA; R— CACAGCCTGGATGGCTACGT), decorin (Dcn: F— GCTGCGGAAATCCGACTTC; R— TTGCCGCCCAGTTCTATGAC), biglycan (Bgn: F— CCTTCCGCTGCGTTACTGA; R—

GCAACCACTGCCTCTACTTCTTATAA), fibromodulin (Fmod: F— GAAGGGTTGTTACGCAAATGG; R— AGATCACCCCCTAGTCTGGGTTA) and lumican (Lum: F— TCCACTTCCAAAGTCCCTGCAAGA; R— AAGCCGAGACAGCATCCTCTTTGA) were used. The amplified cDNA for each individual uninjured or injured patellar tendon sample was analyzed in triplicate with a single negative RT control (0.83 ng total RNA per well) for each sample and each gene. Gene specific efficiencies were calculated using LinRegPCR v7.5 software for each qPCR plate and the relative quantity of mRNA for each gene of interest was computed using the relative gene expression ratios formula, or GED (Gene Expression's CT Difference) [S-Table 1].[23,26] Outliers were removed if their measured expression was greater than two standard deviations from the mean. To test for differences in gene expression, Mann-Whitney tests were used and significance was set at and $p \leq 0.05/2$ and $0.05/2 \leq p \leq 0.1/2$ was considered a trend.

Transmission Electron Microscopy

Tendon bisections were prepared for transmission electron microscopy as previously described.[14] In brief, tendons were fixed with 2.5% glutaraldehyde/4% formaldehyde fixative, post-fixed with osmium tetroxide, dehydrated with ethanol, embedded in Epon 812and polymerized at 60oC. Ultra-thin cross-sections were imaged on JEOL 1400 transmission electron microscope (JEOL Ltd., Tokyo, Japan) equipped with a Gatan Orius widefield side mount CC Digital camera (Gatan Inc., Pleasanton, CA).

Tendon fibril diameter analysis was done as previously described.[14] Briefly, an analysis of tendon diameter in uninjured tissue was done using pooled data from uninjured mice, one tendon from each of five mice of the same genotype and age. Analyses of injured tendons were done using pooled data from 4 to 6 mice of the same genotype and injury state. Five or six digital images from each tendon were taken at 60,000×. Images were analyzed using an RM Biometrics-Bioquant Image Analysis System (Nashville, TN). A region of interest (ROI) of appropriate size was determined within the image so that a minimum of 80 fibrils were measured from each image. Fibril diameters were measured along the minor axis of the fibril cross-section. Tendon diameter measurements were pooled into groups by age and genotype.

Histology and Polarized Light Microscopy

Samples were fixed in formalin, decalcified with Immunocal (Decal Chemical Corporation, Tallman, NY), embedded in paraffin, sectioned into 7 μm slices, stained with Hematoxylin and Eosin, and imaged at 200× with both traditional and polarized light microscopes.

Traditional light images were analyzed with BioQuant software to determine cell density (cells per μm) and cell shape (aspect ratio; 0–1 with 1 being a perfect circle). Polarized light images were analyzed with custom software to quantify collagen fiber alignment, outputted as circular standard deviation. The greater the degrees of circular standard deviation, the less well aligned are the collagen fibers.

For cell-density and cell-shape comparisons, t-tests were used. For circular standard deviation, a parameter which is not normally distributed, Mann-Whitney tests were used. To correct for multiple comparisons, significance was set at and $p \leq 0.05/2$ and $0.05/2 \leq p \leq 0.1/2$ was considered a trend.

Results

Biomechanical Properties

The dynamic modulus |E*| decreased between the uninjured and 3 weeks post-injury for all genotypes across all strains and frequencies [Fig. 1a, 2a, S-Fig. 1; Table 1]. Tanδ, a measure of tendon viscosity, increased 3 weeks post-injury compared to uninjured controls [Fig. 1b, 2b, S-Fig. 1; Table 1]. In WT tendons, no improvement was observed between 3 and 6 weeks post-injury at 4% strain [Fig 1a]. However, an increasing trend was evident for dynamic modulus at 8% strain [Fig. 2a; Table 1]. Tanδ significantly decreased between 3 and 6 weeks at 8% strain [Fig. 2b, Table 1], but not at 4% strain [Fig. 1b, Table 1]. For both |E*| and tanδ, results were intermediate at 6% (Data shown in S-Fig. 1, Table 1).

In $Bgn^{-/-}$ tendons, the changes in |E*| and tanδ between 3 and 6 weeks were similar to those observed in the wild type mice [Fig. 2a,b; Table 1]. However, compared to WT, these mechanical improvements were greater in magnitude and were more consistently statistically significant. Again, changes were not observed at 4% strains [Fig. 1a,b], but there was significant improvement in properties (increasing |E*| and decreasing tanδ) between 3 and 6 weeks at both 6% and 8% strains [Fig. 2a,b; Table 1]. $Dcn^{-/-}$ tendons did not exhibit improved mechanical properties between 3 and 6 weeks post-injury [Fig. 1a,b, 2a,b, S-Fig. 1]. At no strain or frequency was any significant improvement detected for either the dynamic modulus or tanδ [Table 1].

When comparing across genotypes, the uninjured tendons of both knockout genotypes were significantly different from wild type tendons [Fig. 1a,b, 2a,b; Table 2]. At 3 weeks after injury, the biglycan-null tendons had significantly lower dynamic moduli [Fig. 2a] and higher tanδ [Fig. 1b] at 8% strain than the other genotypes. At 6 weeks, this was no longer the case. A summary of dynamic moduli and tanδ values for each genotype is presented in supplemental data S-Fig. 1.

In the analysis of the ramp to failure, the toe and linear moduli appeared to follow the same patterns as the dynamic modulus, but improvement between 3 and 6 weeks post-injury did not reach statistical significance [S-Fig. 2]. Our previous work has demonstrated that the dynamic mechanical parameters |E*| and tanδ are more sensitive measures than static properties to changes resulting from both aging and injury.[13,14,18]

SLRP Expression

For injured wild type tendons, the expression of biglycan was significantly lower than in uninjured tendons [Fig. 3a,b]. Uninjured $Dcn^{-/-}$ expression of biglycan was significantly lower (4.64-fold) than uninjured WT and did not increase at the later time points. Decorin expression was conserved after injury in both wild type and biglycan-null tendons. Uninjured $Dcn^{-/-}$expression of fibromodulin trended higher than uninjured WT (2.7-fold) and injured $Dcn^{-/-}$ tendons (2.7-fold and 2.3-fold, respectively, at 3 and 6 weeks post-injury) [Fig. 3c]. At 3 weeks, lumican expression was higher in $Bgn^{-/-}$ than in WT and at 6 weeks, it was higher in $Bgn^{-/-}$ than in $Dcn^{-/-}$ [Fig. 3d].

Fibril Structure

Collagen fibril diameter distributions were analyzed in uninjured and injured wild type, $Bgn^{-/-}$ and $Dcn^{-/-}$ tendons. using transmission electron microscopy and morphometric analyses [Fig. 4]. The uninjured tendons had similar bimodal distributions across genotypes. However, subtle differences were observed with the wild type tendon have greater overlap of the smaller and larger diameter subpopulation. Both deficient genotypes demonstrated more obvious separation of the smaller diameter (30–60nm) fibril subpopulation. In

addition, in the *Bgn*$^{-/-}$ and *Dcn*$^{-/-}$ tendons the mature, larger diameter subpopulations were shifted to larger and small diameters, respectively. In all injured tendons, a distinct increase in immature, small diameter fibrils (30–60 nm range) was obvious at both 3 and 6 weeks post-injury. This subpopulation is consistent with newly assembled fibrils. Injured wild type tendons demonstrated a broadening and increased number of fibrils in the large diameter subpopulation from 3 to 6 weeks post-injury, consistent with fibril maturation. Injured *Dcn*$^{-/-}$ tendons demonstrated similar changes from 3 to 6 weeks, however, the larger diameter fibril subpopulation was more distinct and shifted to smaller diameters compared to the injured wild type tendons. At 3 an 6 weeks, *Bgn*$^{-/-}$tendons demonstrated decreased numbers of the largest diameter fibrils (>170 nm).

Tenocytes and Fiber Alignment

After injury, cell density is expected to increase, however the apparent changes in Fig 5a only reached statistical significance for *Bgn*$^{-/-}$, with WT and *Dcn*$^{-/-}$ considered a trend [Table 4]. The apparent decrease between 3 and 6 weeks did not reach statistical significance for any genotype. Cell shape appeared to be influenced by injury only in *Dcn*$^{-/-}$ tendons [Fig. 5b], becoming more round after injury. Collagen alignment exhibited a decreasing trend after injury in both WT and Dcn$^{-/-}$ tendons [Fig. 5c]. Interestingly, *Dcn*$^{-/-}$ tendons appears to have improved substantially in this parameter in later healing—no longer different than uninjured by 6 weeks—suggesting that the failure to recapitulate mechanical properties is not caused by a failure to realign.

Discussion

This study investigated the structural, expressional, and mechanical properties of healing tendons deficient in biglycan and decorin. As hypothesized, the ability to recover from injury appears to be moderately impaired in the biglycan- and decorin-null tendons. However, this finding was clearer in the case of the decorin-null tendons than in the biglycan-null. Unlike biglycan-null tendons, there was no mechanical improvement in decorin-null tendons between 3 and 6 weeks post-injury.

Interestingly, while the injured mechanical properties of wild type and decorin-null tendons at 3 weeks post-injury were equivalent, biglycan-null tendons exhibited a significantly lower dynamic modulus and higher tanδ when measured at 8% strain. These data indicate that the absence of biglycan resulted in a deficiency in early stage healing, and therefore a role for biglycan during this period.

In the developing tendon, the temporal shift in gene expression from early dominant biglycan expression which rapidly decreases to sustained decorin expression marks an important transition in the developing tendon.[29] We speculate that a similar shift takes place during the phases of tendon healing. Biglycan expression is known to initially increase after injury[4,21] (measured earlier than in our study). Our data shows that the absence of biglycan adversely affects recently (3 week) injured tendons, and that the absence of decorin adversely affects healing between 3 and 6 weeks post-injury. This evidence suggests that biglycan may play a more prominent role during early healing while decorin may become more prominent in later stages.

In the absence of decorin expression, early healing was not radically altered. It is conceivable that given the reduced mechanics of uninjured decorin null tendons, early healing was actually enhanced, and then plateaued between 3 and 6 weeks. This would be consistent with the broad distribution of mature large diameter fibrils seen at 3 weeks post injury in the decorin null tendon. However, while WT and biglycan-null tendons exhibited some improvement of properties between 3 and 6 weeks after injury, the tendons of decorin-

null mice did not. Given the known role of decorin as a meditator of lateral fibril fusion leading to mature, large diameter tendon collagen fibrils,[5,6,24] it seems reasonable to speculate that decorin's influence during the healing process occurs predominately during the later phases of healing. Interestingly, we have also recently reported that decorin is implicated in the age related structural alterations and mechanical deterioration seen in aging tendons[14] and we speculate that these mechanisms may be related. In the case of the healing tendon between 3 and 6 weeks post-injury, the absence of decorin appears to hinder the mechanical improvement of the tendon. Our data does not suggest that this is directly the result of failure to realign or to regulate collagen fibril synthesis or fusion. It is somewhat surprising that we did not observe substantial differences in fibril distributions across genotypes. Other factors must be responsible for the observed differences in mechanical properties. Additionally, although decorin appears important to latter stage healing, injury did not result in a marked change in decorin expression. Since baseline decorin expression is high, important, but comparatively small changes in decorin expression after injury may be difficult to measure. The cells in $Dcn^{-/-}$ tendons 3 weeks after injury were particularly rounded, likely indicative of more synthetic or proliferative activity.

Interestingly, the expression studies revealed that in the absence of biglycan or decorin, expression of SLRPs fibromodulin and lumican are changed. While ablation of decorin reduced biglycan expression, fibromodulin expression was enhanced in uninjured mice. Additionally, expression of lumican was increased at 3 weeks post-injury in the absence of biglycan, only to decrease to wild type levels by 6 weeks. Previously, regulatory roles for fibromodulin and lumican in tendon fibrillogenesis were described.[15] In addition, synergistic and compensatory mechanisms were suggested for *Bgn* and *Fmod* in tendons.[27] These expression studies provide evidence for compensation by other SLRPs. Further investigations of these relationships are necessary to determine the implications of these potential compensatory mechanisms.

A secondary result of this study was that the differences between the 3 and 6 weeks post-injury states were consistently more pronounced at higher strains. Thus, the structural changes of healing appear to be more influential to mechanics at higher strains. Interestingly, while differences related to injury state are more pronounced at higher strains, we have also observed that differences resulting from age are more pronounced at lower strains.[13,14] This may suggest novel differences in the biology of damage resulting from either aging processes or the repair response to injury.[7] For example, it is possible that higher strains pose a greater risk to healing tendons while prolonged repetitive stress poses a greater risk to the aging tendon.

This study is not without limitations. Our statistical analysis allows us to addresses our specific hypotheses and all p-values are conservatively corrected and provided for the reader to interpret. However, we acknowledge that although subject to other limitations and assumptions, a 4-way ANOVA or mixed effects regression model could offer different benefits. The use of knockout mice does not allow us to fully isolate developmental from current alterations in tendon properties. Additionally, our study design did not allow us to evaluate gene expression immediately after injury, or to see the long term outcome of healed tendon. Moreover, expressional analyses described transcriptional levels. Future investigations will include analyses of protein content and localization. We are currently developing a study featuring conditional knock-out mice to further investigate these mechanisms.

This study offers new insight into the specific regulatory functions of two important molecular constituents of tendon. Results indicate that during healing there is likely a temporal shift in the relative influence of biglycan to decorin. Future work will examine the

influence of advanced aging on the healing process and how the functions of these SLRPs may change throughout an organism's life. As we continue to explore the mechanisms of tendon healing, we move closer to next-generation treatments such as temporally specific biologic factor release, improving medical interventions and surgical outcomes.

Supplementary Material

Refer to Web version on PubMed Central for supplementary material.

Acknowledgments

This study was funded by NIH grant 5R01AR055543 and the Penn Center for Musculoskeletal Disorders (NIH, P30 AR050950). None of the authors have any conflicts of interest to report. We acknowledge Benjamin Freedman for valuable discussions.

References

1. Ameye L, Aria D, Jepsen K, Oldberg A, Xu T, Young MF. Abnormal collagen fibrils in tendons of biglycan/fibromodulin-deficient mice lead to gait impairment, ectopic ossification, and osteoarthritis. FASEB J. 2002; 6:673–80. [PubMed: 11978731]
2. Ansorge HL, Adams S, Birk DE, Soslowsky LJ. Mechanical, compositional, and structural properties of the post-natal mouse Achilles tendon. Ann Biomed Eng. 2011; 39:1904–13. [PubMed: 21431455]
3. Ansorge HL, Adams S, Jawad AF, Birk DE, Soslowsky LJ. Mechanical property changes during neonatal development and healing using a multiple regression model. J Biomech. 2012; 45:1288–92. [PubMed: 22381737]
4. Berglund M, Reno C, Hart DA, Wiig M. Patterns of mRNA expression for matrix molecules and growth factors in flexor tendon injury: differences in the regulation between tendon and tendon sheath. J Hand Surg Am. 2006; 31:1279–1287. [PubMed: 17027787]
5. Birk, DE.; Bruckner, P. Collagen suprastructures. In: Brinckmann, J.; Müller, PK.; Notbohm, H., editors. Topics in Current Chemistry: Collagen. Vol. 247. Springer-Verlag; Berlin: 2005. p. 185-205.
6. Birk DE, Nurminskaya MV, Zycband EI. Collagen fibrillogenesis in situ: fibril segments undergo post-depositional modifications resulting in linear and lateral growth during matrix development. Dev Dyn. 1995; 202:229–43. [PubMed: 7780173]
7. Buckley MR, Dunkman AA, Reuther KE, Kumar A, Pathmanathan L, Beason DP, Birk DE, Soslowsky LJ. Validation of an empirical damage model for aging and in-vivo injury of the murine patellar tendon. J Biomech Eng. 135:041005-1–7. [PubMed: 24231900]
8. Chen S, Birk DE. The regulatory roles of small leucine-rich proteoglycans in extracellular assembly. FEBS J. 2013; 201310.1111/febs.12136
9. Connizzo BK, Sarver JJ, Birk DE, Soslowsky LJ. Effect of age and proteoglycan deficiency on collagen fiber re-alignment and mechanical properties in mouse supraspinatus tendon. J Biomech Eng. 2013; 135(2):021019. [PubMed: 23445064]
10. Corsi A, Xu T, Chen XD, Boyde A, Liang J, Mankani M, Sommer B, Iozzo RV, Eichstetter I, Robey PG, Bianco P, Young MF. Phenotypic effects of biglycan deficiency are linked to collagen fibril abnormalities, are synergized by decorin deficiency, and mimic Ehlers-Danlos-like changes in bone and other connective tissues. J Bone Miner Res. 2002; 17:1180–9. [PubMed: 12102052]
11. Dafforn A, Chen P, Deng G, Herrler M, Iglehart D, Koritala S, Lato S, Pillarisetty S, Purohit R, Wang M, Wang S, Kurn N. Linear mRNA amplification from as little as 5 ng total RNA for global gene expression analysis. BioTechniques. 2004; 37:854–857. [PubMed: 15560142]
12. Dourte LM, Pathmanathan L, Jawad AF, Iozzo RV, Mienaltowski MJ, Birk DE, Soslowsky LJ. Influence of decorin on the mechanical, compositional, and structural properties of the mouse patellar tendon. J Biomech. 2012; 134(3):031005.

13. Dunkman AA, Buckley MR, Mienaltowski MJ, Kumar A, Beason DP, Pathmanathan L, Birk DE, Soslowsky LJ. Dynamic mechanical properties of tendon repair tissue are unaffected by aging. Trans Orthop Res Soc. 2013; 38:614.
14. Dunkman AA, Buckley MR, Mienaltowski MJ, Adams SM, Thomas SJ, Satchell L, Kumar A, Pathmanathan L, Beason DP, Iozzo RV, Birk DE, Soslowsky LJ. Decorin expression is required for age-related changes in tendon structure and mechanical properties. Matrix Biology. 2013; 32:3–13. [PubMed: 23178232]
15. Ezura Y, Chakravarti S, Oldberg A, Chervoneva I, Birk DE. Differential expression of lumican and fibromodulin regulate collagen fibrillogenesis in developing mouse tendons. J Cell Biol. 2000; 151:779–88. [PubMed: 11076963]
16. Favata, M. Paper AAI3246156. 2006. Scarless healing in the fetus: Implications and strategies for postnatal tendon repair. Dissertation available from ProQuest
17. Iozzo RV. The biology of the small leucine-rich proteoglycans. Functional network of interactive proteins. J Biol Chem. 1999; 274:18843–6. [PubMed: 10383378]
18. Kumar A, Dunkman AA, Buckley MR, Pathmanathan L, Mienaltowski MJ, Beason DP, Iozzo RV, Birk DE, Soslowsky LJ. Tendon repair response to injury is affected by the absence of biglycan and decorin. Trans Orthop Res Soc. 2012; 37:158.
19. Leadbetter WB. Cell-matrix response in tendon injury. Clin Sports Med. 1992; 11:533–78. [PubMed: 1638640]
20. Lin TW, Cardenas L, Glaser DL, Soslowsky LJ. Tendon healing in interleukin-4 and interleukin-6 knockout mice. J Biomech. 2006; 39:61–9. [PubMed: 16271588]
21. Lui PP, Cheuk YC, Lee YW, Chan KM. Ectopic chondro-ossification and erroneous extracellular matrix deposition in a tendon window injury model. J Orthop Res. 2012; 301:37–46. [PubMed: 21761446]
22. Lujan TJ, Underwood CJ, Jacobs NT, Weiss JA. Contribution of glycosaminoglycans to viscoelastic tensile behavior of human ligament. J Appl Physiol. 2009; 106:423–31. [PubMed: 19074575]
23. Ramakers C, Ruijter JM, Deprez RH, Moorman AF. Assumption-free analysis of quantitative realtime polymerase chain reaction (PCR) data. Neurosci Lett. 2003; 339:62–6. [PubMed: 12618301]
24. Reed CC, Iozzo RV. The role of decorin in collagen fibrillogenesis and skin homeostasis. Glycoconj J. 2002; 19:249–55. [PubMed: 12975602]
25. Rühland C, Schönherr E, Robenek H, Hansen U, Iozzo RV, Bruckner P, Seidler DG. The glycosaminoglycan chain of decorin plays an important role in collagen fibril formation at the early stages of fibrillogenesis. FEBS J. 2007; 274:4246–55. [PubMed: 17651433]
26. Schefe JH, Lehmann KE, Buschmann IR, Unger T, Funke-Kaiser H. Quantitative real-time RT-PCR data analysis: current concepts and the novel “gene expression’s CT difference” formula. J Mol Med. 2006; 84:901–10. [PubMed: 16972087]
27. Young MF, Bi Y, Ameye L, Chen XD. Biglycan knockout mice: new models for musculoskeletal diseases. Glycoconj J. 2002; 19:257–62. [PubMed: 12975603]
28. Zhang G, Chen S, Goldoni S, Calder BW, Simpson HC, Owens RT, McQuillan DJ, Young MF, Iozzo RV, Birk DE. Genetic evidence for the coordinated regulation of collagen fibrillogenesis in the cornea by decorin and biglycan. J Biol Chem. 2009; 284:8888–97. [PubMed: 19136671]
29. Zhang G, Ezura Y, Chervoneva I, Robinson PS, Beason DP, Carine ET, Soslowsky LJ, Iozzo RV, Birk DE. Decorin regulates assembly of collagen fibrils and acquisition of biomechanical properties during tendon development. J Cell Biochem. 2006; 98:1436–49. [PubMed: 16518859]
30. Zhang G, Young BB, Ezura Y, Favata M, Soslowsky LJ, Chakravarti S, Birk DE. Development of tendon structure and function: regulation of collagen fibrillogenesis. J Musculoskeletal Neuronal Interact. 2005; 5:5–21.

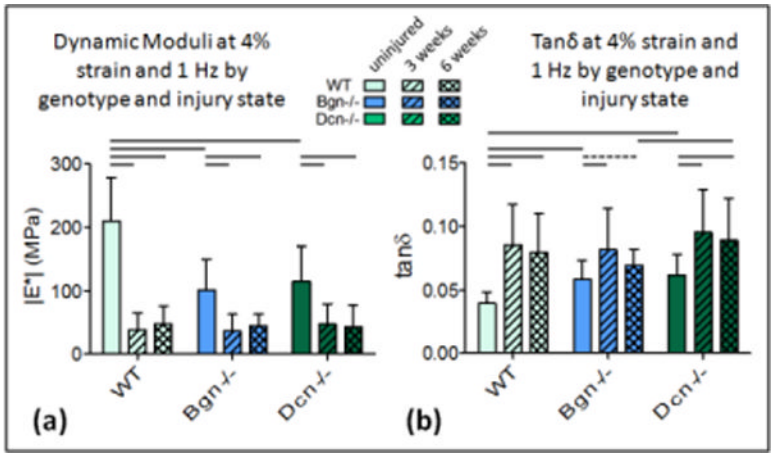

Figure 1.

Dynamic moduli and tanδ at 4% (a) Dynamic modulus decreases after injury in all genotypes. Improvement is not evident between 3 weeks and 6 weeks at this strain. Differences between genotypes in the injured states are not detectable at this strain. (b) Tanδ increases after injury for all genotypes but improvement between 3 and 6 weeks is not detectable at this strain. Tanδ is higher for *Dcn*$^{-/-}$ than WT at 6 weeks. Mean+SD. Significance bars denote $p<0.05/2$; dashed bars denote "trend" $p<0.1/2$.

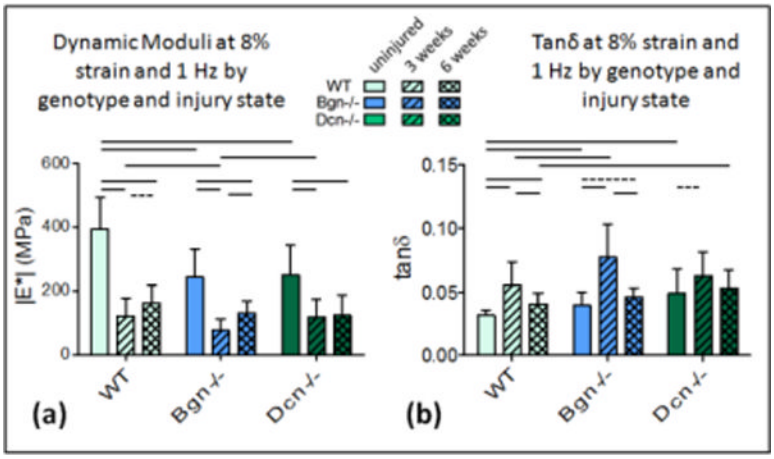

Figure 2.

Dynamic Moduli and Tanδ at 8%. (a) Dynamic modulus decreases after injury in all genotypes. Improvement is evident between 3 and 6 weeks for WT and $Bgn^{-/-}$ but not for $Dcn^{-/-}$. $Bgn^{-/-}$ has a significantly lower dynamic modulus at 3 weeks. (b) Tanδ increases after injury for all genotypes and decreases between 3 and 6 weeks for WT and $Bgn^{-/-}$ but not $Dcn^{-/-}$. Tanδ is higher for $Bgn^{-/-}$ than WT at 3 weeks; higher for $Dcn^{-/-}$ than WT at 6 weeks. Mean+SD. Significance bars denote $p<0.05/2$; dashed bars denote "trend" $p<0.1/2$.

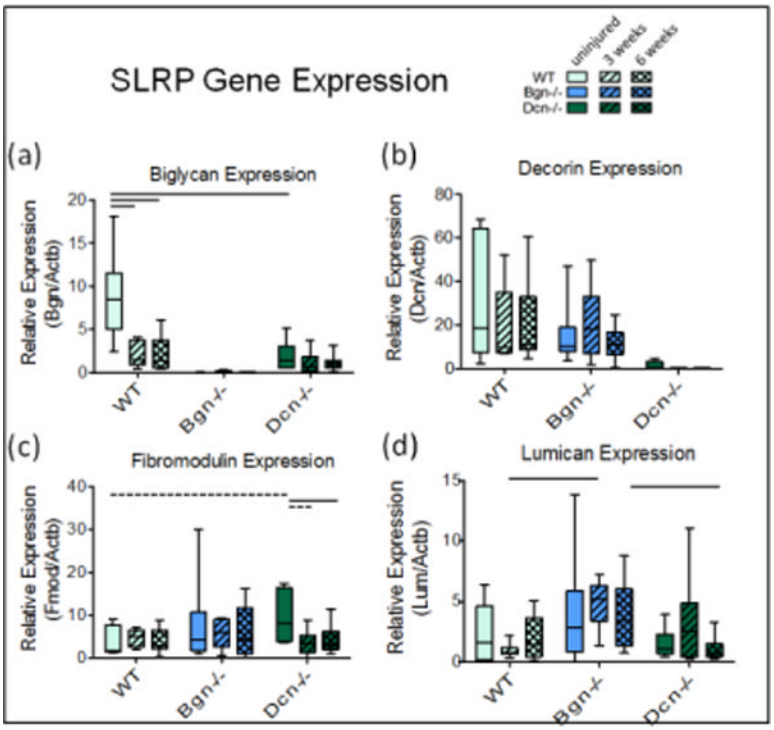

Figure 3.

RT-qPCR for SLRP gene expression. Biglycan (a) and decorin (b) are effectively at background in respective knockouts (significance bars not shown). Uninjured *Dcn*$^{-/-}$ trend towards higher levels of fibromodulin expression (c) and *Bgn*$^{-/-}$ mice may upregulate Lumican relative to WT at 3 weeks post-injury (d). Interquartile range boxes with min-max whiskers.

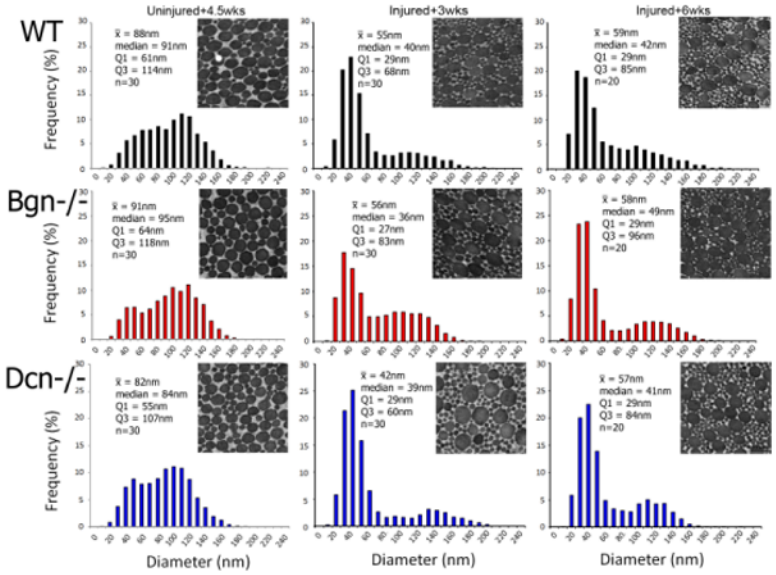

Figure 4.
Fibril Structure. An increase in smaller diameter fibrils is observed after injury, indicating newly assembled fibrils.

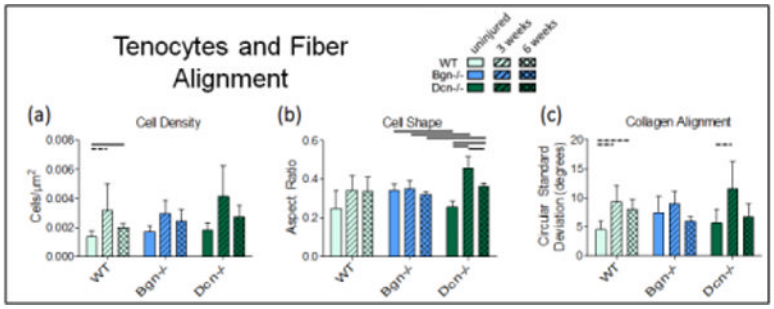

Figure 5.

Tenocytes and Fiber Alignment. (a) Cell density increased after injury but was not significantly decreased between 3 weeks and 6 weeks. (b) Cell shape was apparently only affected by injury in decorin-null tendons. (c) Collagen alignment decreased with injury for WT and *Dcn*−/−. Mean+SD. Bars denote $p<0.05/2$; dashed bars denote "trend" $p<0.1/2$.

Table 1

All calculated *intra*-genotype t-test p-values from dynamic mechanical data.

p≤0.05/2	p≤0.1/2	Wildtype – Dynamic Modulus			Bgn−/− Dynamic Modulus			Dcn−/− Dynamic Modulus		
Strain	**Frequency (Hz)**	**uninj vs 3 wks**	**uninj vs 6 wks**	**3 wks vs 6wks**	**uninj vs 3 wks**	**uninj vs 6 wks**	**3 wks vs 6wks**	**uninj vs 3 wks**	**uninj vs 6 wks**	**3 wks vs 6wks**
4%	**0.01**	<0.001	<0.001	0.174	0.0002	0.0001	0.2684	<0.001	<0.001	0.339
	0.1	<0.001	<0.001	0.193	0.0001	0.0001	0.2072	<0.001	<0.001	0.424
	1	<0.001	<0.001	0.173	0.0001	0.0001	0.1448	<0.001	<0.001	0.380
	5	<0.001	<0.001	0.162	0.0001	0.0001	0.1413	<0.001	<0.001	0.367
	10	<0.001	<0.001	0.162	0.0001	0.0001	0.1458	<0.001	<0.001	0.361
6%	**0.01**	<0.001	<0.001	0.103	<0.001	<0.001	0.0281	<0.001	<0.001	0.439
	0.1	<0.001	<0.001	0.096	<0.001	0.0001	0.0092	<0.001	<0.001	0.459
	1	<0.001	<0.001	0.098	<0.001	0.0001	0.0072	<0.001	<0.001	0.415
	5	<0.001	<0.001	0.096	<0.001	0.0001	0.0066	<0.001	<0.001	0.404
	10	<0.001	<0.001	0.095	<0.001	0.0001	0.0071	<0.001	<0.001	0.399
8%	**0.01**	<0.001	<0.001	0.038	<0.001	0.0001	0.0018	<0.001	<0.001	0.459
	0.1	<0.001	<0.001	0.040	<0.001	0.0001	0.0004	<0.001	<0.001	0.412
	1	<0.001	<0.001	0.033	<0.001	<0.001	0.0004	<0.001	<0.001	0.428
	5	<0.001	<0.001	0.032	<0.001	<0.001	0.0004	<0.001	<0.001	0.437
	10	<0.001	<0.001	0.031	<0.001	<0.001	0.0004	<0.001	<0.001	0.440
		Wildtype – Tanδ			**Bgn−/− Tanδ**			**Dcn−/− Tanδ**		
		uninj vs 3 wks	**uninj vs 6 wks**	**3 wks vs 6wks**	**uninj vs 3 wks**	**uninj vs 6 wks**	**3 wks vs 6wks**	**uninj vs 3 wks**	**uninj vs 6 wks**	**3 wks vs 6wks**
4%	**0.01**	<0.001	<0.001	0.047	0.0165	0.0096	0.4614	<0.001	0.006	0.428
	0.1	<0.001	<0.001	0.314	0.0127	0.0164	0.2663	<0.001	0.005	0.351
	1	<0.001	<0.001	0.319	0.0061	0.0195	0.0921	<0.001	0.003	0.315
	5	<0.001	<0.001	0.272	0.0009	0.0053	0.0573	<0.001	0.003	0.461
	10	<0.001	<0.001	0.239	0.0003	0.0135	0.0220	<0.001	0.002	0.496
6%	**0.01**	<0.001	0.001	0.011	0.0001	0.0330	0.0085	0.019	0.082	0.309
	0.1	<0.001	<0.001	0.064	0.0002	0.0299	0.0059	0.003	0.014	0.343
	1	<0.001	<0.001	0.041	0.0002	0.0181	0.0110	0.006	0.039	0.257
	5	<0.001	<0.001	0.081	<0.001	0.0244	0.0010	0.005	0.023	0.337
	10	<0.001	<0.001	0.187	<0.001	0.0724	0.0004	0.005	0.020	0.281
8%	**0.01**	<0.001	0.004	0.004	<0.001	0.1645	0.0001	0.078	0.336	0.119

p≤0.05/2	p≤0.1/2	Wildtype – Dynamic Modulus			Bgn−/− Dynamic Modulus			Dcn−/− Dynamic Modulus		
Strain	Frequency (Hz)	uninj vs 3 wks	uninj vs 6 wks	3 wks vs 6wks	uninj vs 3 wks	uninj vs 6 wks	3 wks vs 6wks	uninj vs 3 wks	uninj vs 6 wks	3 wks vs 6wks
	0.1	<0.001	<0.001	0.014	<0.001	0.0338	0.0002	0.015	0.071	0.198
	1	<0.001	<0.001	0.007	<0.001	0.0228	0.0001	0.024	0.240	0.071
	5	<0.001	<0.001	0.022	<0.001	0.0141	<0.001	0.009	0.123	0.083
	10	<0.001	<0.001	0.089	<0.001	0.0512	<0.001	0.007	0.099	0.079

Ann Biomed Eng. Author manuscript; available in PMC 2015 March 01.

Table 2

All calculated *inter*-genotype t-test p-values from dynamic mechanical data.

p≤0.05/2	p≤0.1/2	Uninjured – |E*|			3 Weeks – |E*|			6 weeks – E*|		
Strain	**Frequency (Hz)**	**WT vs Bgn−/−**	**WT vs Dcn−/−**	**Bgn−/− vs Dcn−/−**	**WT vs Bgn−/−**	**WT vs Dcn−/−**	**Bgn−/− vs Dcn−/−**	**WT vs Bgn−/−**	**WT vs Dcn−/−**	**Bgn−/− vs Dcn−/−**
4%	**0.01**	<0.001	0.001	0.235	0.781	0.338	0.480	0.792	0.747	0.862
	0.1	<0.001	<0.001	0.489	0.971	0.511	0.512	0.777	0.731	0.859
	1	<0.001	<0.001	0.429	0.845	0.435	0.352	0.721	0.671	0.834
	5	<0.001	<0.001	0.412	0.846	0.408	0.330	0.699	0.656	0.833
	10	<0.001	<0.001	0.391	0.864	0.375	0.317	0.725	0.693	0.858
6%	**0.01**	<0.001	<0.001	0.838	0.353	0.649	0.198	0.419	0.378	0.742
	0.1	<0.001	<0.001	0.927	0.181	0.799	0.135	0.495	0.318	0.567
	1	<0.001	<0.001	0.792	0.135	0.749	0.089	0.444	0.294	0.580
	5	<0.001	<0.001	0.747	0.128	0.722	0.080	0.447	0.292	0.577
	10	<0.001	<0.001	0.722	0.127	0.696	0.079	0.445	0.304	0.599
8%	**0.01**	<0.001	<0.001	0.991	0.062	0.842	0.035	0.146	0.164	0.771
	0.1	<0.001	<0.001	0.887	0.027	0.867	0.031	0.116	0.113	0.638
	1	<0.001	<0.001	0.795	0.024	0.941	0.024	0.081	0.106	0.730
	5	<0.001	<0.001	0.769	0.023	0.970	0.023	0.080	0.109	0.747
	10	<0.001	<0.001	0.752	0.022	0.989	0.022	0.077	0.111	0.767
		Uninjured – tandelta			**3 Weeks – tandelta**			**6 weeks – tandelta**		
		WT vs Bgn−/−	**WT vs Dcn−/−**	**Bgn−/− vs Dcn−/−**	**WT vs Bgn−/−**	**WT vs Dcn−/−**	**Bgn−/− vs Dcn−/−**	**WT vs Bgn−/−**	**WT vs Dcn−/−**	**Bgn−/− vs Dcn−/−**
4%	**0.01**	<0.001	0.001	0.947	0.201	0.546	0.290	0.518	0.244	0.410
	0.1	<0.001	<0.001	0.392	0.155	0.723	0.063	0.107	0.705	0.069
	1	<0.001	<0.001	0.547	0.760	0.444	0.309	0.241	0.480	0.047
	5	<0.001	<0.001	0.923	0.924	0.786	0.861	0.565	0.476	0.153
	10	<0.001	<0.001	0.474	0.802	0.967	0.741	0.519	0.509	0.169
6%	**0.01**	0.004	0.001	0.293	0.824	0.647	0.404	0.201	0.070	0.317
	0.1	0.006	0.001	0.129	0.923	0.859	0.770	0.363	0.153	0.019
	1	0.001	<0.001	0.081	0.665	0.592	0.933	0.691	0.084	0.086
	5	<0.001	<0.001	0.278	0.122	0.545	0.309	0.784	0.134	0.101
	10	<0.001	<0.001	0.441	0.055	0.405	0.271	0.792	0.268	0.086
8%	**0.01**	0.025	0.006	0.299	0.041	0.900	0.032	0.113	0.038	0.340

p≤0.05/2	p≤0.1/2	Uninjured – |E*|			3 Weeks – |E*|			6 weeks – E*|		
Strain	**Frequency (Hz)**	**WT vs Bgn−/−**	**WT vs Dcn−/−**	**Bgn−/− vs Dcn−/−**	**WT vs Bgn−/−**	**WT vs Dcn−/−**	**Bgn−/− vs Dcn−/−**	**WT vs Bgn−/−**	**WT vs Dcn−/−**	**Bgn−/− vs Dcn−/−**
	0.1	0.057	0.005	0.118	0.106	0.552	0.265	0.573	0.020	0.022
	1	0.004	0.001	0.072	0.018	0.309	0.116	0.081	0.012	0.093
	5	0.002	0.001	0.254	0.002	0.202	0.033	0.127	0.052	0.250
	10	0.003	0.001	0.300	0.001	0.171	0.027	0.639	0.156	0.135

Table 3

Mann Whitney p-values from RT-qPCR data.

p≤0.05/2	p≤0.1/2	Biglycan	Decorin	Fmod	Lumican
	uninj vs 3w	0.002	0.445	0.310	0.366
WT	uninj vs 6w	0.002	0.562	0.713	1.000
	3w vs 6w	0.813	0.813	0.492	0.175
	uninj vs 3w	–	0.500	0.828	0.199
Bgn−/−	uninj vs 6w	–	0.624	0.683	0.665
	3w vs 6w	–	0.214	0.818	0.307
	uninj vs 3w	0.272	–	0.038	0.366
Dcn−/−	uninj vs 6w	0.451	–	0.019	0.393
	3w vs 6w	0.595	–	0.928	0.174
	WT vs Bgn−/−	–	0.374	0.511	0.473
uninj	WT vs Dcn−/−	0.005	–	0.035	0.836
	Bgn−/− vs Dcn −/−	–	–	0.132	0.242
	WT vs Bgn−/−	–	0.758	0.562	0.001
3w	WT vs Dcn−/−	0.174	–	0.445	0.234
	Bgn−/− vs Dcn−/−	–	–	0.193	0.270
	WT vs Bgn−/−	–	0.249	0.767	0.079
6w	WT vs Dcn−/−	0.418	–	0.751	0.212
	Bgn−/− vs Dcn−/−	–	–	0.926	0.006

Table 4

Histology p-values from t-tests (density and cell shape) and Mann Whitney (circ st. dev.).

p≤0.05/2		Wild Type	
p≤0.1/2	uninj vs 3 wks	uninj vs 6 wks	3 wks vs 6wks
Density	0.051	0.015	0.127
Cell Shape	0.082	0.088	0.467
Circ. St. Dev.	0.032	0.032	0.343
		Bgn−/−	
	uninj vs 3 wks	uninj vs 6 wks	3 wks vs 6wks
Density	0.011	0.063	0.204
Cell Shape	0.337	0.167	0.099
Circ. St. Dev.	0.196	0.095	0.057
		Dcn−/−	
	uninj vs 3 wks	uninj vs 6 wks	3 wks vs 6wks
Density	0.041	0.047	0.133
Cell Shape	0.001	0.001	0.012
Circ. St. Dev.	0.036	0.278	0.057
		Uninjured	
	WT vs Bgn−/−	WT vs Dcn−/−	Bgn−/− vs Dcn−/−
Density	0.223	0.183	0.656
Cell Shape	0.110	0.899	0.011
Circ. St. Dev.	0.151	0.690	0.310
		3 Weeks	
	WT vs Bgn−/−	WT vs Dcn−/−	Bgn−/− vs Dcn−/−
Density	0.839	0.546	0.351
Cell Shape	0.833	0.080	0.036
Circ. St. Dev.	0.857	0.629	0.400
		6 weeks	
	WT vs Bgn−/−	WT vs Dcn−/−	Bgn−/− vs Dcn−/−
Density	0.387	0.120	0.587
Cell Shape	0.651	0.554	0.014
Circ. St. Dev.	0.114	0.486	0.886